PHOTOSYNTHETICA 47 (4): 567-574, 2009

The reduced S_{-1} and S_{-2} oxidation states of the O_2-evolving complex of photosystem II: An EPR microwave power saturation study

D. KOULOUGLIOTIS

Technological Educational Institute (T.E.I.) of Ionian Islands, Department of Environmental Technology and Ecology, 2 Calvou Sq., 29100, Zakynthos, Greece[*]
Institute of Materials Science, NCSR "Democritos", 15310 Aghia Paraskevi Attikis, Athens, Greece

Abstract

Progressive microwave power saturation ($P_{1/2}$) measurements have been performed on the tyrosine D radical ($Y_D^\bullet$) of photosystem II (PSII) in order to examine its relaxation enhancement by the oxygen-evolving complex (OEC) poised to the reduced S_{-1} and S_{-2} oxidation states by NO treatment. Analysis of the power saturation curves showed that the S_{-1} oxidation state of the OEC does not enhance the relaxation of $Y_D^\bullet$: it therefore possesses a diamagnetic ground state. In contrast, the Mn(II)-Mn(III) multiline electron paramagnetic resonance (EPR) signal characteristic of the S_{-2} oxidation state of the OEC was shown to provide a relaxation enhancement pathway for $Y_D^\bullet$, however less efficient relative to the one provided by the S_2-state multiline EPR signal. We also examined the $Y_D^\bullet$ relaxation enhancement characteristics of the EPR-silent oxidation state produced after brief (1–5 min) dark incubation at 0°C of a PSII sample poised to the EPR-active S_{-2} state. This EPR-silent oxidation state denoted as "0°C incubation" state was shown to possess remarkably similar $P_{1/2}$ values with the EPR-active S_{-2} state in the overall examined temperature range (6–20 K). In addition, these values remained unchanged after successive cycles of the OEC between the EPR-active S_{-2} state and the "0°C incubation" state. The data presented in this work point to the conclusion that the "0°C incubation" state is indeed an S_{-2} oxidation state with half-integer spin.

Additional keywords: oxygen-evolving complex; photosystem II; power saturation; reduced S-states.

Introduction

The O_2-evolving complex (OEC) of photosystem II (PSII), composed of a tetranuclear Mn cluster and a Ca^{2+} ion, catalyzes photosynthetic water oxidation to molecular oxygen. Catalysis is achieved by advancement of the OEC (or the Mn-cluster as noted otherwise) through five intermediate oxidation states known as S_i-states (i = 0–4) in four light-driven sequential one-electron oxidation steps. Oxygen evolves during the S_4 to S_0 transition. A special chlorophyll (Chl) moiety known as P_{680} is photooxidized to P_{680}^+ upon initial light absorption and subsequently the electron is transferred *via* a pheophytin (Pheo) molecule to the primary (Q_A) and secondary (Q_B) plastoquinone electron acceptors. The precise nature of the primary electron donor, P_{680}, is still not well understood, with the current experimental evidence pointing to a weakly coupled complex of four monomeric chlorophylls over which the excited state tends to be delocalized (Murray and Barber 2007). A tyrosine radical (Tyr 161 of the D1 polypeptide) known as $Y_Z^\bullet$ mediates electron transfer from the OEC to P_{680}^+ *via* a series of $S_iY_Z^\bullet$ metalloradical intermediates (Goussias *et al.* 2002, Diner and Rappaport 2002, Barber 2003, Petrouleas *et al.* 2005, Ioannidis *et al.* 2006, McEvoy and Brudvig 2006). In addition to Y_Z, another tyrosine residue (Tyr160 of the D2 polypeptide) known as Y_D is located symmetrically to Y_Z (Koulougliotis *et al.* 1995) and exists in the form

Received 22 May 2009; *accepted* 11 November 2009.
[*]Present addres; fax: 30-2695024949, e-mail: dkoul@teiion.gr
Abbreviations: Chl – chlorophyll; CW EPR – Continuous Wave Electron Paramagnetic Resonance; MeOH – methanol; MES – 2-[N-morpholineethane sulfonic acid]; OEC – O_2-evolving complex; $P_{1/2}$ – microwave power at half saturation; PSII – photosystem II; S-states – S_{-5}…..S_4 oxidation states of the OEC; Y_D – redox-active tyrosine 160 on the D2 polypeptide of PSII; $Y_D^\bullet$ – tyrosine D radical localized on Tyr160 of the D2 polypeptide of PSII; Y_Z – redox-active tyrosine 161 on the D1 polypeptide of PSII; $Y_Z^\bullet$ – tyrosine Z radical localized on Tyr161 of the D1 polypeptide of PSII.
Acknowledgements: D.K. wishes to thank Dr. Vasili Petrouleas for access to the EPR instrument of the Institute of Materials Science at NCSR "Democritos" and helpful discussions and the TMR Programme of the European Union for a research fellowship (Contr. No. ERBFMBICT983239).

of a stable neutral radical, $Y_D^\bullet$. Due to its remarkable stability, $Y_D^\bullet$ has been studied by several magnetic resonance techniques and a lot of information has been obtained concerning its location, spin density, kinetics, pH dependency, orientation, local environment and possible physiological role (Rutherford *et al.* 2004 and references therein). More specifically, the relaxation behavior of $Y_D^\bullet$ has been studied by several groups by using continuous wave (CW) and pulsed EPR techniques at cryogenic temperatures. Some of these studies aimed at quantifying the long range pairwise dipolar interaction between $Y_D^\bullet$ and other paramagnets of PSII (non-heme Fe, OEC) (Innes and Brudvig 1989, Hirsh *et al.* 1992, Kodera *et al.* 1992, Kodera *et al.* 1994, Koulougliotis *et al.* 1995, Koulougliotis *et al.* 1997, Mamedov *et al*. 2004).

In other studies, the examination of the relaxation behavior $Y_D^\bullet$ has given valuable information regarding the magnetic properties of the different S-states of the OEC (Styring and Rutherford 1988, Evelo *et al.* 1989, Koulougliotis *et al.* 1992, MacLachlan *et al.* 1994, Koulougliotis *et al.* 1997, Peterson *et al.* 1999, Peterson *et al.* 2003, Åhrling and Peterson 2003, Ho *et al.* 2007). Some specific findings of these studies are the following: The different S states (S_0, S_1, S_2 and S_3) possess different potency as relaxers with the potency series being modulated by temperature (Styring and Rutherford 1988, Evelo *et al.* 1989, Peterson *et al.* 1999). For example at 4.3 K the microwave power at half-saturation ($P_{1/2}$) of $Y_D^\bullet$ is lower when the OEC is poised to the S_2 state relative to its value when the OEC is poised to the S_0 state [$P_{1/2}$ (S_2) < $P_{1/2}$ (S_0)]. This series is inverted at temperatures higher than 20 K, where $P_{1/2}$ (S_2) > $P_{1/2}$ (S_0). At this point, it is interesting to point out that direct measurements of the $P_{1/2}$ values of the multiline EPR signals exhibited by the S_0 and S_2 states of the Mn-cluster as a function of temperature show qualitatively the same trend with the $P_{1/2}$ values of the $Y_D^\bullet$ radical with the cluster poised to the corresponding states (Peterson *et al*. 1999). The examination of the relaxation behavior of $Y_D^\bullet$ *via* saturation-recovery EPR (Koulougliotis *et al.* 1992) has also shown that the S_1-resting state of the OEC is diamagnetic in its ground state, while the S_1-active state of the cluster is paramagnetic.

Both pulsed and CW EPR spin relaxation measurements have also been performed on the different multiline EPR signals originating from the S_0 and S_2 states of the OEC in order to obtain direct information concerning their magnetic properties (Pace *et al.* 1991, Lorigan and Britt 1994, Koulougliotis *et al.* 1997, Peterson *et al.* 1999, Lorigan and Britt 2000, Geijer *et al.* 2001, Peterson *et al.* 2003, Kulik *et al.* 2005a, Kulik *et al.* 2005b).

In addition to the S_0, S_1, S_2 and S_3 oxidation states of the OEC, considerable effort has been done to produce and follow spectroscopically lower (more reduced) oxidation states of the OEC in PSII. The interest for the study of these lower oxidation states (S_i, i = –1, –5) of the Mn-cluster derives from their possible connection with the process of its photoassembly and photoactivation (Ananyev *et al.* 2001). Different reductants have been used in order to obtain these states such as hydrazine (Messinger *et al.* 1997, Messinger *et al.* 2001, Razeghifard *et al.* 2005, Shevela *et al.* 2006), hydroxylamine (Bouges 1971, Beck *et al.* 1987, Kretschmann *et al.* 1993, Riggs-Gelasco *et al.* 1996, Messinger *et al.* 2001), hydrogen peroxide (Velthuys *et al.* 1978, Mano *et al.* 1987), hydrogen sulfide (Sivaraja *et al*. 1988) and more recently NO (Ioannidis *et al.* 1998, Schansker *et al.* 2002, Sarrou *et al.* 2003). Recent studies have provided experimental evidence that over-reduced states of the Mn-cluster can also be induced *in vivo* after treatments that do not involve the use of exogenous reductants (Quigg *et al.* 2003, Higuchi *et al.* 2003).

Focusing on the studies employing NO, we pointed our attention to the fact that there is strong experimental evidence that NO acts as a reductant of the dark stable S_1 state of the OEC which finally reaches an oxidation state characterized by a multiline EPR signal ascribed to a Mn(II)-Mn(III) dimanganese complex (Sarrou *et al.* 1998). During its reaction with the OEC, NO acts stepwise so that the Mn-cluster passes progressively *via* the S_0 and S_{-1} EPR states (Ioannidis *et al.* 1998). Recent studies have assigned the Mn(II)-Mn(III) multiline EPR signal to an S_{-2} oxidation state of the OEC by combining experimental evidence from flash oxymetry, chlorophyll *α* fluorescence and EPR spectroscopy (Schansker *et al.* 2002). The EPR multiline Mn(II)-Mn(III) EPR signal presents an interesting and so far unexplained behavior as a function of incubation temperature: it appears at maximum intensity after incubation at the specific temperature of –30°C, completely disappears after brief incubation (less than a minute) at 0°C and reappears without loss of intensity after a relatively short incubation period (ca 30 min) at –30°C. The question of whether the "0°C incubation" EPR silent form of the OEC is an S state identical to the one yielding the Mn(II)-Mn(III) multiline EPR signal is not answered definitively in the literature, even though the so far existing observations "rule out the possibility of a reversible oxidation-reduction process occurring during the EPR-active-to-EPR-silent conversion" (Schansker *et al.* 2002).

In the current work, the CW EPR technique of microwave power saturation was employed in order to obtain information on the magnetic properties of the S_{-1} oxidation state of the OEC, the S_{-2} oxidation state of the complex charactrerized by the Mn(II)-Mn(III) multiline EPR signal and the "0°C incubation" EPR silent oxidation state which is in thermal equilibrium with the EPR active S_{-2} state. More specifically, we studied the effect of these three states of the OEC on the relaxation properties of the $Y_D^\bullet$ radical, a technique which as described above has been successfully employed in the past for probing the magnetic properties of the higher oxidation states of the Mn cluster.

Materials and methods

PSII membranes were prepared from market spinach leaves as described elsewhere (Berthold *et al.* 1981, Ford and Evans 1983). Samples for EPR measurements were suspended in a buffer containing 0.4 M sucrose, 15 mM NaCl, 40 mM MES-NaOH (pH 6.5) and their final concentration was 3-5 mg(Chl) cm^{-3}. Sample illumination was performed with a 340 W projection lamp filtered through a saturated solution of $CuSO_4$. When needed, the PSII membranes were subjected to long-term dark adaptation (3–4 h in an ice-water bath) followed by freezing at 77 K in complete darkness, in order to ensure a homogeneous population of the OEC in the diamagnetic S_1-resting state (Koulougliotis *et al*. 1992). Samples were poised to the paramagnetic S_1-active state by illumination at 0°C for 6 min followed by the dark incubation at 0°C for 20 min and immediate freezing at 77 K (Koulougliotis *et al*. 1992). The S_2-state was achieved by continuous illumination at 200 K for 4 min.

NO treatment was achieved by bubbling in darkness at 0–4°C with different NO/N_2 mixtures under nitrogen atmosphere for a short time period (1–2 min) followed by immediate freezing at 77 K. The samples were subsequently incubated at –30°C for variable time periods. Addition of methanol (MeOH) in a 3% v/v concentration before the NO treatment was employed in order to obtain a PSII sample in which the OEC is poised mainly to the S_{-1} oxidation state (Ioannidis *et al*. 1998). Removal of NO in the end of the incubation period was achieved by bubbling of pure N_2 gas for a few (2–5) min. The EPR derivative signal intensity (I) of the resonance of $Y_D^{\bullet}$ was measured as the height between the first peak (g = 2.0107) and the left baseline, as shown in the inset (*B*) of Fig. 1.

EPR measurements at liquid He temperatures were obtained with an *ER-200D-SRC* spectrometer (*Bruker*, Karlsruhe, Germany) interfaced to a personal computer and equiped with an *ESR 900* cryostat (Oxford, Oxfordshire, UK), a 035M NMR gaussmeter (*Bruker*, Karlsruhe, Germany) and a *MF76A* frequency counter (*Anritsu*, Tokyo, Japan).

The empirical equation used to express the effect of the progressive power saturation on an inhomogeneously broadened EPR derivative signal intensity (I) is the following (Rupp *et al*. 1978):

$$I = \frac{I_0 \sqrt{P}}{(1 + P/P_{1/2})^{b/2}} \qquad (1)$$

where b is the inhomogeneity parameter varying between b=1 (completely inhomogeneous line broadening) and b=3 (completely homogeneous line broadening), I_0 corresponds to the unsaturated signal intensity, P is the applied microwave power and $P_{1/2}$ is the microwave power at half-saturation. $P_{1/2}$ is proportional to $1/T_1T_2$, where $1/T_1$ and $1/T_2$ are the spin-lattice and spin-spin relaxation rates, respectively. Consequently, the determination of $P_{1/2}$ provides a measure of the relaxation characteristics of the observed species, even though the temperature dependence obtained cannot discriminate between T_1 and T_2 effects. Eq. 1 may be rewritten in the following form:

$$log\left(\frac{I}{\sqrt{P}}\right) = log\, I_0 - \left(\frac{b}{2}\right) log\left(1 + P/P_{1/2}\right) \qquad (2)$$

In the present study, the experimental variable $log\left(\frac{I}{\sqrt{P}}\right)$ was plotted as a function logP. A representative data set, corresponding to T = 10 K, is shown in Fig. 1*A*. Subsequently, the theoretical expression of Eq. 2 was employed in order to obtain the best fit to the experimental data points. I_0 and $P_{1/2}$ were used as fitting parameters, while the value parameter b was set constant and equal to 1 in all fits. Data fitting was accomplished by using the nonlinear curve fitting routine of the program *Microcal Origin 7.0* (Northhampton, MA, USA). This program uses the Levenberg-Marquardt algorithm in an iterative process in order to determine the fitting parameter values that minimize the deviation of the theoretical curve from the experimental points. The algorithm combines the Gauss-Newton and steepest descent methods for achieving chi-square minimization. The fitting process produces as output the best parameter values (I_0, $P_{1/2}$) accompanied with a fitting error which is a measure of the deviation between the theory and experiment. The values of the $P_{1/2}$ parameter extracted from the theoretical fits presented a fitting error with a typical value of 7–10% in all measurements. Each $P_{1/2}$ determination was repeated several times (usually three) by using different sample preparations. The standard deviation of the obtained average $P_{1/2}$ value from the independent experiments represents an additional error which will be noted as data scattering. In the following figures the error bars on the data depict either the total error (fitting error plus data scattering) or only the fitting error. In the latter case (depiction of the fitting error only), the data points from two equivalent experiments are presented. This is done in order to provide a graphic representation of the two error sources and to stress the importance of the data reproducibility between independent sample preparations.

In this work, the observed species is the stable tyrosine $Y_D^{\bullet}$ radical. We have examined the (liquid He) temperature dependence of its $P_{1/2}$ value by poising the OEC of PSII to the following three different oxidation states: the EPR active S_{-2} oxidation state (Mn(II)-Mn(III) multiline), the "0°C incubation" EPR silent oxidation state which is in thermal equilibrium with the EPR active S_{-2} oxidation state and the EPR silent S_{-1} oxidation state. The selective population of the majority of the PSII

centers in these respective states was performed *via* NO reduction by following the earlier published protocol (Ioannidis *et al.* 1998) and also described analytically in the Results section.

Results

Relaxation behavior of $Y_D^\bullet$ with the OEC poised to the S_{-2} oxidation state: The Mn(II)-Mn(III) multiline EPR signal, characteristic of the S_{-2} oxidation state of the OEC, was induced at its maximum intensity by overnight (total of 10–12 h) dark incubation at –30°C of relatively dilute PSII membranes [3–5 mg(Chl) cm^{-3}] treated with NO/N_2 mixtures of 2:5 or 3:5. Under these circumstances, the yield of the Mn(II) – Mn(III) multine signal was consistently maximal. Fig. 1*A* shows a typical saturation curve obtained for $Y_D^\bullet$ in a PSII sample poised to the S_{-2} oxidation state. The theoretical fit to the experimental data (by using Eq. 2) is depicted as a continuous line. The inset of the same figure (Fig. 1*B*) depicts the CW EPR spectrum of $Y_D^\bullet$ at nonsaturating microwave power, in addition to the peak height that was used for the measurement of the signal intensity.

In Fig. 2 the $P_{1/2}$ values of $Y_D^\bullet$ for PSII samples poised to the S_{-2} (characterized by the Mn(II)-Mn(III) multiline EPR signal), the S_1-resting and the S_2 oxidation states of the OEC are shown in the 6–20 K temperature range. These values will be denoted as $P_{1/2}(S_{-2})$, $P_{1/2}(S_1$-resting) and $P_{1/2}(S_2)$ in the rest of the paper. The error bars on the data represent the total error (data scattering from 3 independent experiments plus fitting error) as explained in detail in Materials and methods.

It can be seen that the Mn(II)-Mn(III) multiline EPR signal is a less potent relaxation enhancer relative to the S_2-state multiline EPR signal. However, its effect relative to the diamagnetic S_1-resting state is significant and becomes larger as the temperature raises. In fact, the $P_{1/2}(S_{-2})$ values for $Y_D^\bullet$ are very similar with those obtained in PSII samples with the OEC poised to the paramagnetic S_1-active state (data not shown).

The relaxation behavior of $Y_D^\bullet$ was also examined in PSII samples where the Mn(II)-Mn(III) multiline signal was first produced at its maximum and a brief dark incubation (5 min) at 0°C was subsequently performed. This treatment results in practically complete loss of the Mn(II)-Mn(III) EPR signal (Goussias *et al.* 1997, Sarrou *et al*. 1998). These $P_{1/2}$ values (denoted as $P_{1/2}(0^oC)$) extracted from the fits to Eq. 2 are shown in Fig. 3. In the same figure, the $P_{1/2}(S_{-2})$ values which correspond to the presence of the Mn(II)-Mn(III) multiline EPR signal are also shown for comparison. The data presented correspond to two independent representative experiments and cover the 6–20 K temperature region. The error bars correspond to the uncertainty involved in the extraction of the $P_{1/2}$'s from the fitting of the saturation curves (noted as fitting error in Materials and methods). As noted in Fig. 3, the $P_{1/2}(0^oC)$ and the $P_{1/2}(S_{-2})$ values are

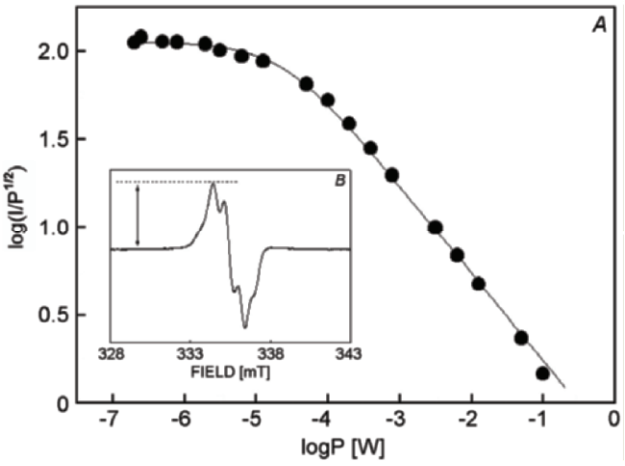

Fig. 1. *A*: Progressive microwave power saturation of the $Y_D^\bullet$ radical with the O_2-evolving complex poised to the S_{-2}-Mn(II)-Mn(III) multiline redox state. The experimental data were obtained at 10 K. The theoretical fit to the experimental data (*solid line*) was done by using Eq. 2 for b = 1. The $P_{1/2}$ value extracted from the shown fit is $P_{1/2}$ = (23 ± 2) μW. *B* (inset): The CW EPR spectrum of the $Y_D^\bullet$ radical observed with the O_2-evolving complex poised to the S_{-2}-Mn(II)-Mn(III) multiline redox state, under non-saturating conditions. The *double arrow* depicts the peak height that was used for the measurement of the signal intensity (I). Experimental conditions: temperature 10 K, microwave frequency 9.41 GHz, field-modulation amplitude 0.4 mT, microwave power 4 μW, field-modulation frequency 100 KHz.

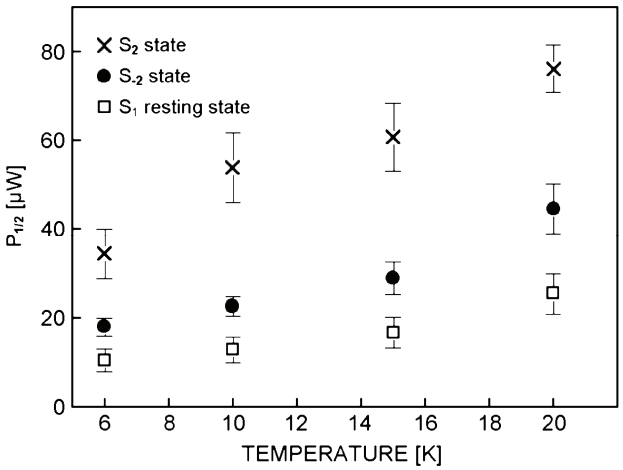

Fig. 2. Temperature dependence of the microwave power at half-saturation ($P_{1/2}$) of the $Y_D^\bullet$ radical with the O_2-evolving complex poised to the S_1-resting (□), S_{-2}-Mn(II)-Mn(III) multiline (●) and S_2-multiline (×) redox states. The data presented are the average of three independent experiments and the error bars correspond to the total error (data scattering in addition to fitting error).

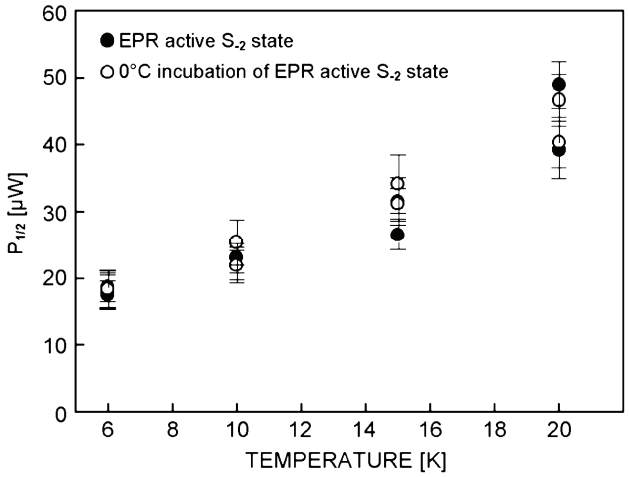

Fig. 3. Temperature dependence of the microwave power at half-saturation ($P_{1/2}$) of the $Y_D^\bullet$ radical with the O_2-evolving complex poised to the Mn(II)-Mn(III) multiline state produced at its maximum after dark incubation in the presence of NO at –30°C (●) and after brief incubation (5 min) of the sample at 0°C (○). The data presented correspond to two different samples. The error bars correspond to the fitting error.

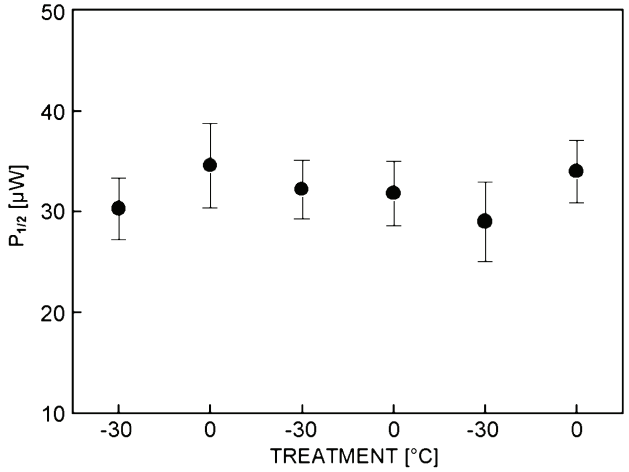

Fig. 4. $P_{1/2}$ values of the $Y_D^\bullet$ radical with the O_2-evolving complex interconverting between the EPR-active S_{-2} state characterized by the Mn(II)-Mn(III) multiline signal induced by incubation at –30°C and the EPR-silent state induced after brief incubation at 0°C. The $P_{1/2}$ values shown were measured at 15 K and correspond to the average of two independent experiments. The error bars correspond to the total error (data scattering in addition to fitting error).

identical within experimental error in the overall examined temperature range, which leads to the conclusion that the relaxation behavior of $Y_D^\bullet$ is not affected by the specific treatment (*i.e.* brief dark incubation of S_{-2} state at 0°C) of the OEC.

The –30°C (EPR-active) – 0°C (EPR-silent) dark incubation steps were repeated several times (up to 4) on the same sample and the $P_{1/2}$ behavior of $Y_D^\bullet$ was examined at two temperatures (6 and 15 K) after each

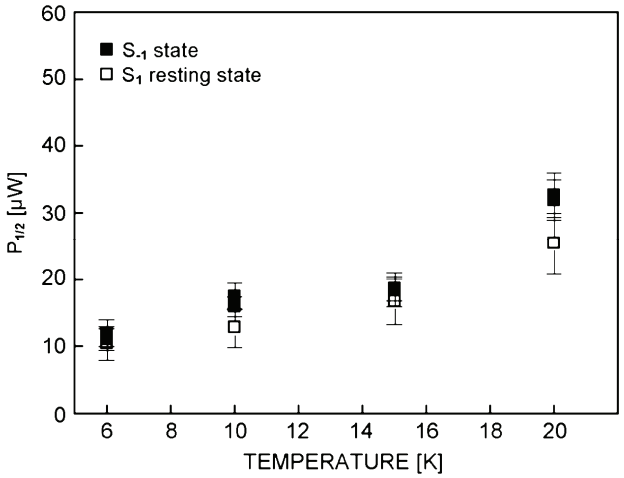

Fig. 5. Temperature dependence of the microwave power at half-saturation ($P_{1/2}$) of the $Y_D^\bullet$ radical with the O_2-evolving complex poised to the S_1-resting (□) and the S_{-1} (■) states. The data on the S_{-1}-state are from two independent data sets with their error bars corresponding to the fitting error. The data on the S_1-resting state are the averages of three independent experiments with their error bars corresponding to the total error (data scattering in addition to fitting error).

treatment. The results obtained at 15 K (averages of two independent experiments in different samples) are reported in Fig. 4. The error bars represent the total error, *i.e.* the addition of the data scattering and the fitting error (*see* Materials and methods). It can be seen that throughout the cycles the $P_{1/2}$ value of $Y_D^\bullet$ remains stable within experimental error, which is what was observed at 6 K as well (data not shown). Thus, the reversibility of the treatment is reflected in the relaxation behavior of $Y_D^\bullet$ and consequently the magnetic properties of the OEC as well.

The results presented above indicate that the conversion of the Mn-cluster from the EPR-active S_{-2} oxidation state to an EPR-silent form following a brief incubation at 0°C does not affect its magnetic properties. The Mn-cluster maintains its paramagnetism in the "0°C incubation" oxidation state and is therefore able to provide a relaxation enhancement pathway for $Y_D^\bullet$, even though it is EPR-silent.

Relaxation behavior of $Y_D^\bullet$ with the OEC poised to the S_{-1} state: As described earlier (Ioannidis *et al.* 1998), dark incubation at –30°C of NO-treated PSII membranes in the presence of 3% (v/v) MeOH resulted initially to the formation of the EPR signal of the S_0 state followed by its disappearance after prolonged incubation (9 h). The experimental evidence provided in that same work argues for this EPR-silent state being the S_{-1} oxidation state of the OEC. In the present work, a similar treatment was performed in order to produce the S_{-1} state and then examine how the relaxation behavior of $Y_D^\bullet$ is affected. The experiment was repeated several times with different PSII preparations and total incubation times ranging from

10 to 14 h. Assuring reproducibility in the results is essential for the specific experiments since most probably the percentage of centers populating the S_{-1} state is variable. The data showed remarkable reproducibility and two representative data sets are presented in Fig. 5. The error bars correspond to the fitting error during the extraction of the $P_{1/2}$ values.

Together with the $P_{1/2}$ values (for temperatures ranging between 6 and 20 K) obtained for the S_{-1} state, the ones for the S_1-resting state (same as in Fig. 2) are also shown in Fig. 5 for comparison purposes. The two data sets (S_{-1} and S_1-resting states) are identical within experimental error. This provides strong experimental evidence for the S_{-1} state of the OEC possessing a diamagnetic ground state.

By combining the experiments presented in the two sections above, we note that the two EPR-silent states examined – the S_{-1} state and the "0^oC incubation" state being in thermal equilibrium with the EPR-active S_{-2} state – are very different regarding their magnetic properties: the first is diamagnetic and the latter paramagnetic. In addition, the latter two states ("0°C incubation" and S_{-2}) possess remarkably similar paramagnetism. Therefore, the herein presented data provide strong experimental evidence that the EPR-silent "0°C incubation" state is indeed an S_{-2} oxidation state with half-integer spin.

Discussion

In this work the CW EPR technique of microwave power saturation was employed in order to obtain information on the magnetic properties of the lower oxidation S_{-1} and S_{-2} states of the OEC in PSII. These states were attained by NO reduction for long time periods (> 10 h). The percentage of PSII centers poised to the S state of interest is an issue that needs to be discussed at this point. In fact, it has to be noted that the $P_{1/2}$ value obtained by fitting a power saturation curve with Eq. 2 is an apparent $P_{1/2}$ value. This apparent value is certainly "largely determined by the dominant S-population in the sample" (Styring and Rutherford 1988); it however provides an under- or overestimation of the actual $P_{1/2}$ value corresponding to the pure S state of interest.

First we concentrate on the apparent $P_{1/2}$ values presented in Fig. 5 (*full symbols*) which were obtained in a sample with the OEC poised to the S_{-1} oxidation state. This sample was poised to this EPR-silent state after prolonged treatment with NO (>10 h) in the presence of methanol. Previous studies (Ioannidis *et al.* 1998) provide an estimate of at least 65% of the centers being in the S_{-1} oxidation state after this treatment, with the rest of the centers shared mainly between the S_0 and the S_{-2} states. The latter two minority states (S_0 and S_{-2}) are paramagnetic and they possess $P_{1/2}$ values that are quite larger than the apparent values shown for the S_{-1} state. By examining *e.g.* the values at T = 6 K, one can notice the following: it is known that at T = 6 K the S_0 state multiline signal relaxes faster than the S_2-state multiline signal (Peterson *et al.* 1999) and in accordance to that, $P_{1/2}$ measurements $Y_D^\bullet$ at the same temperature range have shown that $P_{1/2}(S_0) > P_{1/2}(S_2)$ (Styring and Rutherford 1988). By taking into account the $P_{1/2}(S_2)$ measurements of $Y_D^\bullet$ presented in this work (Fig. 2), one concludes that at T = 6 K the $P_{1/2}(S_0)$ value of $Y_D^\bullet$ is expected to be larger than 35 μW, *i.e.* a factor of 3 larger (at least) from the apparent $P_{1/2}$ value of $Y_D^\bullet$ corresponding to the S_{-1} state. The $P_{1/2}(S_{-2})$ measurements of $Y_D^\bullet$ presented in Fig. 2, also show that at T = 6 K the $P_{1/2}(S_{-2})$ value is almost a factor of 2 larger that the apparent $P_{1/2}(S_{-1})$ value. From the above, one reaches the conclusion that the apparent $P_{1/2}(S_{-1})$ values shown in Fig. 5 provide an overestimation of the actual $P_{1/2}(S_{-1})$ values that would be obtained in a hypothetical sample with 100% population of the S_{-1} state. This argument enhances the validity of our result that the S_{-1} state of the OEC in PSII possesses a diamagnetic ground state.

In the following, we focus our discussion to the results obtained concerning the S_{-2} oxidation state of the OEC. According to earlier studies (Ioannidis *et al.* 1998), the NO treatment used to obtain the maximal intensity of the S_{-2} state characteristic Mn(II)-Mn(III) multiline EPR signal results to at least 60% population of the PSII centers at this EPR-active S_{-2} oxidation state. The rest of the centers seems to be mainly in the S_{-1} oxidation state. The current work showed however that the S_{-1} state of the Mn-cluster is diamagnetic at the temperature range examined. Thus, the apparent $P_{1/2}(S_{-2})$ values of $Y_D^\bullet$ plotted in Fig. 2 provide an underestimation of the actual $P_{1/2}(S_{-2})$ values. In the current work, the apparent $P_{1/2}(S_{-2})$ values of $Y_D^\bullet$ were measured in order to serve as a basis for comparison with the apparent $P_{1/2}(0^oC)$ values of $Y_D^\bullet$ (Fig. 3). The remarkable similarity of these two data sets (Fig. 3) in all the examined temperatures, which was always reproduced in different PSII preparations, shows that the EPR silent oxidation state obtained after brief 0°C dark incubation of the S_{-2} state enhances the relaxation of $Y_D^\bullet$ with the same potency as does the EPR-active S_{-2} oxidation state. In other words, the "0°C incubation" and the S_{-2} oxidation states possess similar magnetic properties, at least as these are probed *via* the microwave power saturation measurements. In addition, successive cycles of incubation between –30°C and 0°C reproduce very similar values of $P_{1/2}(S_{-2})$ and $P_{1/2}(0°C)$ respectively, as shown in Fig. 4. This remarkable reversibility in the $P_{1/2}$ values implies that the OEC maintains its structural integrity during the EPR-active-to-EPR-silent interconversion. Consequently, the EPR-silent "0°C incubation" form of the OEC does represent a major fraction of the PSII centers and corresponds to an S_{-2} oxidation state, maintaining its potential physiological relevance with the process of photoactivation.

References

Åhrling, K.A., Peterson, S.A.: Light adaptation of photosystem II is mediated by the plastoquinone pool. – Biochem. **42**: 7655-7662, 2003.

Ananyev, G.M., Zaltsman, L., Vasko, C., Dismukes, G.C.: The inorganic biochemistry of photosynthetic oxygen evolution/ water oxidation. – Biochim. Biophys. Acta **1503**: 52-68, 2001.

Barber, J.: Photosystem II: the engine of life. – Quart. Rev. Biophys. **36**: 71-89, 2003.

Beck, W.F., Brudvig, G.W.: Reactions of hydroxylamine with the electron-donor side of photosystem II. – Biochem. **26**: 8285-8295, 1987.

Berthold, D.A., Babcock, G.T., Yocum, C.F.: A highly resolved, oxygen-evolving photosystem II preparation from spinach thylakoid membranes. EPR and electron-transport properties. – FEBS Lett. **134**: 231-234, 1981.

Bouges, B.: Action of low concentrations of hydroxylamine on oxygen evolved by Chlorella and spinach chloroplasts. – Biochim. Biophys. Acta **234**: 103-112, 1971.

Diner, B.A., Rappaport, F.: Structure, dynamics, and energetics of the primary photochemistry of photosystem II of oxygenic photosynthesis. – Annu. Rev. Plant Biol. **53**: 551-580, 2002.

Evelo, R.G., Styring, S., Rutherford, A.W., Hoff, A.J.: EPR relaxation measurements of photosystem II reaction centers: influence of S-state oxidation and temperature. – Biochim. Biophys. Acta – Bioenergetics **973:** 428-442, 1989.

Ford, R.C., Evans, M.C.W.: Isolation of a photosystem-2 preparation from higher plants with highly enriched oxygen evolution activity. – FEBS Lett. **160**: 159-164, 1983.

Geijer, P., Peterson, S., Åhrling, K.A., Deák, Z., Styring, S.: Comparative studies of the S_0 and S_2 multiline electron paramagnetic resonance signals from the manganese cluster in Photosystem II. – Biochim. Biophys. Acta-Bioenergetics **1503**: 83-95, 2001.

Goussias, C., Boussac, A., Rutherford, A.W.: Photosystem II and photosynthetic oxidation of water: an overview. – Philos. Trans. R. Soc. London **357**: 1369-1381, 2002.

Goussias, C., Ioannidis, N., Petrouleas, V.: Low-temperature interactions of NO with the S1 and S2 states of the water-oxidizing complex of photosystem. 2. A novel Mn-multiline EPR signal derived from the S_1 state. – Biochem. **36**: 9261-9266, 1997.

Higuchi, M., Noguchi, T., Sonoike, K.: Over-reduced states of the Mn-cluster in cucumber leaves induced by dark-chilling treatment. – Biochim. Biophys. Acta **1604**: 151-158, 2003.

Hirsh, D.J., Beck, W.F., Innes, J. B., Brudvig, G.W.: Using saturation-recovery EPR to measure distances in proteins - applications to photosystem II. – Biochem. **31**: 532-541, 1992.

Ho, F.M., Morvaridi, S.F., Mamedov, F., Styring, S.: Enhancement of $Y_D^{\bullet}$ spin relaxation by the $CaMn_4$ cluster in photosystem II detected at room temperature: A new probe for the S-cycle. – Biochim. Biophys. Acta-Bioenergetics **1767**: 5-14, 2007.

Innes, J. B., Brudvig, G.W.: Location and magnetic relaxation properties of the stable tyrosine radical in photosystem II. – Biochem. **28**: 1116-1125, 1989.

Ioannidis, N., Sarrou, J., Schansker, G., Petrouleas, V.: NO reversibly reduces the water-oxidizing complex of photosystem II through S_0 and S_1 to the state characterized by the Mn(II)-Mn(III) multiline EPR signal. – Biochem. **37**: 16445-16451, 1998.

Ioannidis, N., Zahariou, G., Petrouleas, V.: Trapping of the S2 to S3 state intermediate of the oxygen-evolving complex of photosystem II. – Biochem. 45:, 6252-6259, 2006.

Kodera, Y., Dzuba, S.A., Hara, H., Kawamori, A.: Distances from tyrosine D+ to the manganese cluster and the acceptor iron in Photosystem II as determined by selective hole burning in EPR spectra. – Biochim. Biophys. Acta-Bioenergetics 1186: 91-99, 1994.

Kodera, Y., Takura, K., Kawamori, A.: Distance of P680 from the manganese complex in photosytem II studied by time resolved EPR. – Biochim. Biophys. Acta-Bioenergetics **1101**: 23-32, 1992.

Koulougliotis, D., Hirsh, D.J., Brudvig, G.W.: The O_2-evolving center of Photosystem II is diamagnetic in the S_1 resting state. – J. Am. Chem. Soc. **114**: 8322-8323, 1992.

Koulougliotis, D., Tang, X.-S., Diner, B.A., Brudvig, G.W.: Spectroscopic evidence for the symmetrical location of tyrosine D and tyrosine Z in photosystem II. – Biochem. **34**: 2850-2856, 1995.

Koulougliotis, D., Schweitzer, R.H., Brudvig, G.W.: The tetranuclear manganese cluster in photosystem II: Location and magnetic properties of the S2 state as determined by saturation-recovery EPR spectroscopy. – Biochem. **36**: 9735-9746, 1997.

Kretschmann, H., Witt, H.T.: Chemical reduction of the water splitting enzyme system of photosynthesis and its light-induced reoxidation characterized by optical and mass spectroscopic measurements: A basis for the estimation of the states of the redox active manganese and of water in the quaternary oxygen-evolving S-state cycle. – Biochim. Biophys. Acta-Bioenergetics **1144**: 331-345, 1993.

Kulik, L.V., Epel, B., Lubitz, W., Messinger, J.: 55Mn pulse ENDOR at 3 GHz of the S0 and S2 states of the oxygen evolving complex in photosystem II. – J. Am. Chem. Soc. **127**: 2392-2393, 2005a.

Kulik, L.V., Lubitz, W., Messinger, J.: Electron spin-lattice relaxation of the S0 state of the oxygen-evolving complex in photosystem II and of dinuclear manganese model complexes. – Biochem. **44**: 9368-9374, 2005b.

Lorigan, G.A., Britt, R.D.: Temperature-dependent pulsed electron-paramagnetic-resonance studies of the S2 state nultiline signal of the photosynthetic oxygen-evolving complex. – Biochem. **33**: 12072-12076, 1994.

Lorigan, G.A., Britt, R.D.: Electron spin-lattice relaxation studies of different forms of the S2 state multiline EPR signal of the Photosystem II oxygen-evolving complex. – Photosynth. Res. **66**: 189-198, 2000.

MacLachlan, D.J., Nugent, J.H.A., Bratt, P.J., Evans, M.C.W.: The effects of calcium depletion on the O_2-evolving complex in spinach PSII: The S_1^*, S_2^* and S_3^* states and the role of the 17 kDa and 23 kDa extrinsic polypeptides. – Biochim. Biophys. Acta-Bioenergetics **1186**: 186-200, 1994.

Mamedov, F., Smith, P.J., Styring, S., Pace, R.J.: Relaxation behaviour of the tyrosine YD radical in photosystem II: evidence for strong dipolar interaction with paramagnetic centers in the S1 and S2 states. – Phys. Chem. Chem. Phys. **6**: 4890-4896, 2004.

Mano, J., Takahashi, M., Asada, K.: Oxygen evolution from hydrogen peroxide in photosystem II: Flash-induced catalytic activity of water-oxidizing photosytem II membranes. – Biochem. **26**: 2495-2501, 1987.

McEvoy, J.P., Brudvig, G.W.: Water-splitting chemistry of photosystem II. – Chem. Rev. **106**: 4455-4483, 2006.

Messinger, J., Seaton, G., Wydrzynski, T., Wacker, U., Renger, G.: S-3 state of the water oxidase in photosystem II. – Biochem. **36**: 6862-6873, 1997.

Messinger, J., Robblee, J.H., Bergmann, U., Fernandez, C., Glatzel, P., Isgandarova, S., Hanssum, B., Renger, G., Crammer, S.P., Yachandra, V.K.: Manganese oxidation states of Photosystem II. – Proceeding of the 12th International Congress on Photosynthesis, CSIRO Publishing, Collingwood, Australia. Pp. S10-S19, 2001.

Murray, J.W., Barber, J.: Structural characteristics of channels and pathways in photosystem II including the identification of an oxygen channel. – J. Struct. Biol. **159:** 228-237, 2007.

Pace, R.J., Smith, P., Bramley, R., Stehlik, D.: EPR saturation and temperature dependence studies on signals from the oxygen-evolving center of photosystem II. – Biochim. Biophys. Acta-Bioenergetics **1058**: 161-170, 1991.

Peterson, S., Åhrling, K.A., Styring, S.: The EPR signals from the S_0 nad S_2 states of the Mn cluster in photosystem II relax differently. – Biochem. **38**: 15223-15230, 1999.

Peterson, S., Åhrling, K.A, Högblom, J.E., Styring, S.: Flash-induced relaxation changes of the EPR signals from the manganese cluster and Y_D reveal a light-adaptation process of photosystem II. – Biochem. **42**: 2748-2758, 2003.

Petrouleas, V., Koulougliotis, D., Ioannidis, N.: Trapping of metalloradical intermediates of the S-states at liquid helium temperatures. Overview of the phenomenology and mechanistic implications. – Biochem. **44**: 6723-6728, 2005.

Quigg, A., Beardall, J., Wydrzynski, T.: Photoacclimation involves modulation of the photosynthetic oxygen-evolving reactions in *Dunaliella tertiolecta* and *Phaeodactylum tricornutum*. – Funct. Plant Biol. **30**: 301-308, 2003.

Razeghifard, M.R., Kuzek, D., Pace, R.J.: EPR kinetic studies of the S_1 state in spinach thylakoids. – Biochim. Biophys. Acta-Bioenergetics **1708**: 35-41, 2005.

Riggs-Gelasco, P.J., Mei, R., Yocum, C.F., Penner-Hahn, J.E.: Reduced derivatives of the Mn cluster in the oxygen-evolving complex of photosystem II: an EXAFS study. – J. Amer. Chem. Soc. **118**: 2387-2399, 1996.

Rupp, H., Cammack, R, Rao, K.K., Hall, D.O., Cammack, R.: Electron-spin relaxation of iron-sulphur proteins studied by microwave power saturation. – Biochim. Biophys. Acta **537**: 255-269, 1978.

Rutherford, A.W., Boussac, A., Faller, P.: The stable tyrosyl radical in Photosystem II: why D? – Biochim. Biophys. Acta-Bioenergetics **1655**: 222-230, 2004.

Sarrou, J., Ioannidis, N., Deligiannakis, Y., Petrouleas, V.: A Mn(II)-Mn(III) EPR signal arises from the interaction of NO with S1 the state of the water-oxidizing complex of photosystem II. – Biochem. **37**: 3581-3587, 1998.

Sarrou, J., Isgandarova S., Kern, J., Zouni, A., Renger, G., Lubitz, W., Messinger, J.: Nitric oxide-induced formation of the S_2 state in the oxygen-evolving complex of photosystem II from *Synechococcus elongatus*. – Biochem. **42**: 1016-1023, 2003.

Schansker, G., Goussias, C., Petrouleas, V., Rutherford, A.W.: Reduction of the Mn cluster of the water-oxidizing enzyme by nitric oxide: Formation of an S_2 state. – Biochem. **41**: 3057-3064, 2002.

Shevela, D.N., Khorobrykh, A.A., Klimov, V.V.: Effect of bicarbonate on the water-oxidizing complex of photosystem II in the super-reduced S-states. – Biochim. Biophys. Acta-Bioenergetics **1757**: 253-261, 2006.

Sivaraja, M., Hunziker, D., Dismukes, G.C.: The reaction of H_2S with the photosynthetic water-oxidizing complex and its lack of reaction with the primary electron acceptor in spinach. – Biochim. Biophys. Acta **936**: 228-235, 1988.

Styring, S.A., Rutherford, A.W.: The microwave power saturation of $SII_{s\,low}$ varies with the redox state of the oxygen-evolving complex in photosystem II. – Biochem. **27**: 4915-4923, 1988.

Velthuys, B.R., Kok, B.: Photosynthetic oxygen evolution from hydrogen peroxide. – Biochim. Biophys. Acta-Bioenergetics **502**: 211-221, 1978.